

FINITE ELEMENT ANALYSIS OF FREE CONVECTION IN A SQUARE CAVITY WITH MAGNETIC FIELD AND SEMI CIRCULAR HEAT SOURCE OF DIFFERENT ORIENTATIONS

P. Naga Lakshmi Devi¹, S. Saroja², Dr. M. Subrahmanya Sreenivasa Rao³, Dr. P. J. Ravindranath⁴

Assistant Professor, Malla Reddy Engineering college (Autonomous), Hyderabad, Telangana, India.

Associate Professor, Malla Reddy Engineering college (Autonomous), Hyderabad, Telangana, India.

Assistant Professor, Department of Mechanical Engineering, VNRVJIET, Hyderabad, Telangana, India.

Associate Professor, Avanthi Institute of Engineering and Technology, Hyderabad, Telangana, India.

ABSTRACT: the present study we discuss the effects of MHD free convection on heat flow within a square cavity. Free convection flow in the presence of magnetic field in a square cavity with semi circular heat source was studied in this chapter. The lower wall of cavity was heated from below and upper wall of cavity was cold whereas side walls of the cavity were thermally insulated., Finite Element Method has been used to convert the non-linear coupled partial differential equations for flow and temperature field into a matrix form of equations, which can be solved iteratively with the help of a computer code. The Galerkin Finite Element Method of three noded triangular elements is used to divide the physical domain into smaller segments, which is a pre-requisite for finite element method. Numerical results are presented in terms of stream functions, isotherms, temperature profiles and Nusselt numbers.

Keywords: MHD free convention, Magnetic field,

I.INTRODUCTION

Free convection in cavity has received considerable attention from researchers. Most of the cavities commonly used in industries are circular, square, rectangular, trapezoidal and triangular etc. Square cavities have received a considerable attention for its application in various fields. Taghikhani and Chavoshi [1] numerically investigated two dimensional magneto hydrodynamics (MHD) free convection with internal heating in a square cavity. They observed that the effect of the magnetic field is to reduce the convective heat transfer inside the cavity. Bakhshan and Ashoori [2] investigated numerically analysis of a fluid behavior in a rectangular enclosure under the effect of magnetic field. They observed that

Nusselt number rises with increasing Grashof and Prandtl numbers and decreasing Hartmann and orientation of magnetic field. Öztop and Al-Salem [3] numerically investigated effects of joule heating on MHD natural convection in non-isothermally heated enclosure. They observed that positive stream functions are decreased with increasing of Hartmann number and thermal boundary layer becomes larger. Parvin and Nasrin [4] investigated numerically analysis of the flow and heat transfer characteristics for MHD free convection in an enclosure with a heated obstacle. They found that buoyancy-induced vortex in the streamlines is increased and thermal layer near the heated surface becomes thick with increasing Rayleigh number. Natural convection in a square cavity localized heating from below was investigated by Santosh et al. [5]. They observed that heat transfer increases when the heater source is placed towards the cold wall. In the light of the above literatures,

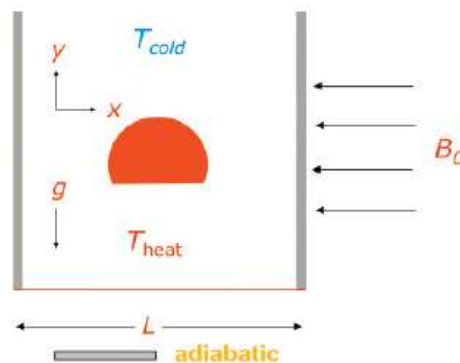


Fig.1: Schematic diagram of the physical system.

II.MATHEMATICAL FORMULATION:

A schematic diagram of the system considered in present study is shown in Fig. 1. The system consists of a square cavity with sides of length L and a semi-circular solid block is located at the centre of the enclosure. The left and right walls are considered to be adiabatic. The top wall is kept at a constant temperature T_c . The bottom wall and semi-circular obstacle are assumed to be uniform temperature be T_h . Here T_c is less than T_h . The uniform magnetic field B_0 is also applied to the fluid in the direction parallel to y . Based on the model, two dimensional, laminar, incompressible steady equations are written by considering a uniform applied magnetic field. The gravitational force (g) acts in the vertically downward direction. We assumed that Boussinesq approximation is valid and radiation mode of the heat transfer and Joule heating are neglected. Thus, using the coordinate system shown in Fig. 1, the governing equations can be written in dimensional form

$$\frac{\partial u}{\partial x} + \frac{\partial v}{\partial y} = 0 \quad (3.1)$$

$$\rho \left(u \frac{\partial v}{\partial x} + v \frac{\partial v}{\partial y} \right) = -\frac{1}{\rho} \frac{\partial p}{\partial y} + \nu \left(\frac{\partial^2 v}{\partial x^2} + \frac{\partial^2 v}{\partial y^2} \right) + g\beta(T - T_c) - B_0^2 v \quad (3.2)$$

$$u \frac{\partial T}{\partial x} + v \frac{\partial T}{\partial y} = \alpha \left(\frac{\partial^2 T}{\partial x^2} + \frac{\partial^2 T}{\partial y^2} \right) \quad (3.3)$$

with boundary conditions

$$u(x, 0) = u(x, L) = u(0, y) = u(L, y) = 0,$$

$$v(x, 0) = v(x, L) = v(0, L) = v(L, y) = 0,$$

$$T(x, 0) = T_h,$$

$$\frac{\partial T}{\partial y}(x, L) = 0, \quad T(0, y) = T_h - (T_h - T_c) \frac{y}{L},$$

The Continuity equation (3.1) can be satisfied automatically by introducing the stream function ' ψ ' as

$$u = \frac{\partial \psi}{\partial y} \quad (3.4a)$$

$$v = -\frac{\partial \psi}{\partial x} \quad (3.4b)$$

where x and y are the distances measured along the horizontal and vertical directions respectively u and v are the velocity components in the x and y directions respectively T denotes the temperature ν and α are kinematic viscosity and thermal diffusivity respectively P is the pressure and ρ is the density T_h and T_c are the temperatures at hot bottom wall and cold vertical wall respectively L is the side of the square cavity.

Using the following non dimensional variables,

$$\text{Width} \quad X = \frac{x}{L}$$

$$\text{Height} \quad Y = \frac{y}{L}$$

$$\text{Velocity components} \quad \begin{cases} U = \frac{uL}{\alpha} \\ V = \frac{vL}{\alpha} \end{cases}$$

$$\text{Stream function} \quad \bar{\psi} = \frac{\psi}{\alpha}$$

$$\text{Pressure} \quad P = \frac{pL^2}{\rho\alpha^2}$$

$$\text{Prandtl Number} \quad \text{Pr} = \frac{\nu}{\alpha}$$

$$\text{Hartmann Number} \quad Ha^2 = \frac{B_0^2 L^3}{\mu}$$

$$\text{Rayleigh number} \quad Ra = \frac{g\beta(T_h - T_c)L^3 \text{Pr}}{\nu^2}$$

$$\text{Temperature} \quad \theta = \frac{T - T_c}{T_h - T_c}$$

The governing equations (3.1)-(3.3) reduce to non-dimensional form as

$$U \frac{\partial U}{\partial X} + V \frac{\partial V}{\partial Y} = 0 \quad (3.5)$$

$$U \frac{\partial V}{\partial X} + V \frac{\partial V}{\partial Y} = -\frac{\partial P}{\partial Y} + \text{Pr} \left(\frac{\partial^2 V}{\partial X^2} + \frac{\partial^2 V}{\partial Y^2} \right) + Ra \text{Pr} \theta - Ha^2 \text{Pr} V \quad (3.6)$$

$$U \frac{\partial \theta}{\partial X} + V \frac{\partial \theta}{\partial Y} = \left(\frac{\partial^2 \theta}{\partial X^2} + \frac{\partial^2 \theta}{\partial Y^2} \right) \quad (3.7)$$

with the non dimensionless boundary conditions are

$$U(X, 0) = U(X, 1) = U(0, Y) = U(1, Y) = 0,$$

$$V(X, 0) = V(X, 1) = V(0, Y) = V(1, Y) = 0,$$

$$\theta(X, 0) = 1, \quad \frac{\partial \theta}{\partial Y}(X, 1) = 0,$$

where X and Y are dimensionless coordinates varying along horizontal and vertical directions respectively U and V are dimensionless velocity components in the X and Y directions respectively θ is the dimensionless temperature P is the dimensionless pressure Ra and Pr are Rayleigh Prandtl numbers respectively.

III.SOLUTION OF PROBLEM

Thus far we have derived the partial differential equations, which describe the heat and fluid flow behavior in the vicinity of porous medium. The development of governing equations is one part but the second and important part is to solve these equations in order to predict the various parameters of interest in the porous medium. There are various numerical methods available to achieve the solution of these equations, but the most popular numerical methods are Finite difference method, Finite volume method and the Finite element method. The selection of these numerical methods is an important decision, which is influenced by variety of factors amongst which the geometry of domain plays a vital role. Other factors include the ease with which these partial differential equations can be transformed into simple forms, the computational time required and the flexibility in development of computer code to solve these equations. In the present study, we have predominantly used Finite Element Method (FEM). The following sections enlighten the Finite element method and present its application to solve the above-mentioned equations.

The Finite Element Method is a deservedly popular method amongst scientific community. This method was originally developed to study the mechanical stresses in a complex airframe structure popularized by Zienkiewicz and Cheung (23) by applying it to continuum mechanics. Since then the application of Finite Element Method has been exploited to solve the numerous problems in various engineering disciplines. The great thing about finite element method is its ease with which it can be generalized to myriad engineering problems comprised of different materials.

Another admirable feature of the Finite Element Method (FEM) is that it can be applied wide range of geometries having irregular boundaries, which is highly difficult to achieve with other contemporary methods. FEM can be said to have comprised of roughly 5 steps to solve any particular problem. The steps can be summarized as

- **Descritizing the domain:** This step involves the division of whole physical domain into smaller segments known as elements, and then identifying the nodes, coordinates of each node and ensuring proper connectivity between the nodes.
- **Specifying the equation:** In this step, the governing equation is specified and an equation is written in terms of nodal values
- **Development of Global matrix:** The equations are arranged in a global matrix which takes into account the whole domain
- **Solution:** The equations are solved to get the desired variable at each table in the domain
- **Evaluate the quantities of interest:** After solving the equations a set of values is obtained for each node, which can be further processed to get the quantities of interest.

There are varieties of elements available in FEM, which are distinguished by the presence of number of nodes. The present study is carried out by using a simple 3-noded triangular element as shown in fig. 2

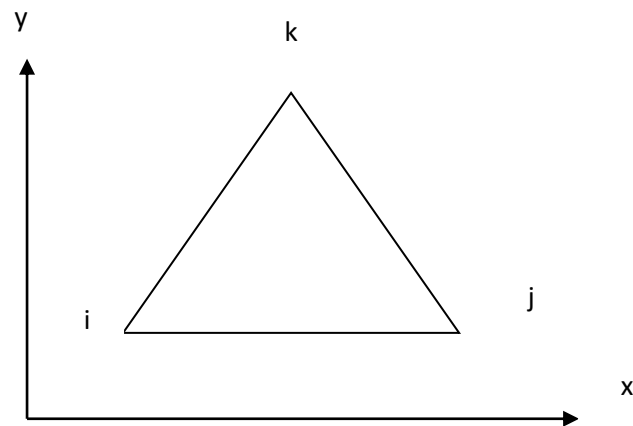


Fig.2: Typical triangular element

Let us consider that the variable to be determined in the triangular area is ' θ '. The polynomial function for ' θ ' can be expressed as:

$$\theta = \alpha_1 + \alpha_2 x + \alpha_3 y \quad (1)$$

The variable θ has the value θ_i , θ_j and θ_k at the nodal position i, j, and k of the element. The x and y coordinates at these points are x_i , x_j , x_k and y_i , y_j and y_k respectively. Substitution of these nodal values in the equation (1) helps in determining the constants α_1 , α_2 , α_3 which are:

$$\alpha_1 = 1/2A [(x_j y_k - x_k y_j) \theta_i + (x_k y_i - x_i y_k) \theta_j + (x_i y_j - x_j y_i) \theta_k] \quad (2)$$

$$\alpha_2 = 1/2A [(y_j - y_k) \theta_i + (y_k - y_i) \theta_j + (y_i - y_j) \theta_k] \quad (3)$$

$$\alpha_3 = 1/2A [(x_k - x_j) \theta_i + (x_i - x_k) \theta_j + (x_j - x_i) \theta_k] \quad (4)$$

where A is area of the triangle given as

$$2A = \begin{vmatrix} 1 & x_i & y_i \\ 1 & x_j & y_j \\ 1 & x_k & y_k \end{vmatrix} \quad (5)$$

Substitution of $\alpha_1, \alpha_2, \alpha_3$ in the equation (1) and mathematical arrangement of the terms results into

$$\theta = N_i \theta_i + N_j \theta_j + N_k \theta_k \quad (6)$$

In equation (6), N_i, N_j and N_k are the shape function given by

$$N_m = \frac{a_m + b_m x + c_m y}{2A}, \quad m = i, j, k \quad (7)$$

The constants can be expressed in terms of coordinates as

$$a_i = x_j y_k - x_k y_j$$

$$b_i = y_j - y_k \quad (8a)$$

$$c_i = x_k - x_j$$

$$a_j = x_k y_i - x_i y_k$$

$$b_j = y_k - y_i \quad (8b)$$

$$c_j = x_i - x_k$$

$$a_k = x_i y_j - x_j y_i$$

$$b_k = y_i - y_j \quad (8c)$$

$$c_k = x_j - x_i$$

The triangular element can be subdivided into three triangles with a point in the center of original triangle as shown in fig.3.

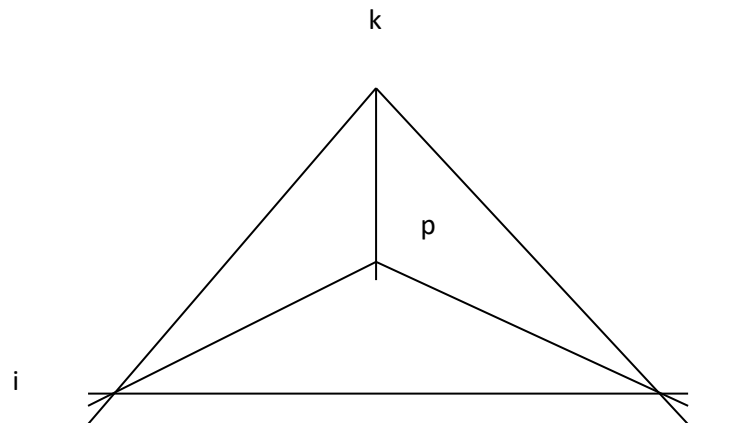


Fig.3: showing the sub triangular areas

Defining the new area ratios as

$$L_1 = \frac{\text{area } pij}{\text{area } ijk} \quad (9a)$$

$$L_2 = \frac{\text{area } pj k}{\text{area } ijk} \quad (9b)$$

$$L_3 = \frac{\text{area } pki}{\text{area } ijk} \quad (9c)$$

It can be shown that

$$L_1 = N_1 \quad (10a)$$

$$L_2 = N_2 \quad (10b)$$

$$L_3 = N_3 \quad (10c)$$

Good insight into the FEM is given in Segerlind [24], Galerkin method is employed to convert the partial differential equations into matrix form for an element. The steps invented are as given below. Please note that the nodal terms i, j & k are replaced by 1,2 & 3 respectively in subsequent discussions for simplicity.

The momentum and energy balance equations are solved using the Galerkin finite element method. Continuity equation will be used as a constraint due to mass conservation and this constraint may be used to obtain the pressure

distribution. In order to solve equations, we use the finite element method where the pressure P is eliminated by a penalty parameter γ and the incompressibility criteria

$$P = -\gamma \left(\frac{\partial U}{\partial X} + \frac{\partial V}{\partial Y} \right)$$

(3.8)

The continuity equation (3.5) is automatically satisfied for large values of γ .

Using equation (3.8) and introducing stream function, the momentum equation (3.6) reduce to

$$\left[\frac{\partial \bar{\psi}}{\partial Y} \frac{\partial^2 \bar{\psi}}{\partial X \partial Y} - \frac{\partial \bar{\psi}}{\partial X} \frac{\partial^2 \bar{\psi}}{\partial Y^2} \right] = \gamma \left(\frac{\partial^2 \bar{\psi}}{\partial Y^2} \frac{\partial \bar{\psi}}{\partial X} + \frac{\partial^2 \bar{\psi}}{\partial Y^2} \right) + \text{Pr} \left[\frac{\partial^2 \bar{\psi}}{\partial X^2} + \frac{\partial^2 \bar{\psi}}{\partial Y^2} \right] - Ra \text{Pr} \theta + Ha^2 \text{Pr} \frac{\partial \bar{\psi}}{\partial Y}$$

(3.10)

Application of Galerkin method to equation (3.10) yields:

$$\{R^e\} = - \int_A N^T \left\{ \begin{array}{l} \left[\frac{\partial \bar{\psi}}{\partial Y} \frac{\partial^2 \bar{\psi}}{\partial X \partial Y} - \frac{\partial \bar{\psi}}{\partial X} \frac{\partial^2 \bar{\psi}}{\partial Y^2} \right] - \gamma \left(\frac{\partial^2 \bar{\psi}}{\partial Y^2} \frac{\partial \bar{\psi}}{\partial X} + \frac{\partial^2 \bar{\psi}}{\partial Y^2} \right) \\ - \text{Pr} \left[\frac{\partial^2 \bar{\psi}}{\partial X^2} + \frac{\partial^2 \bar{\psi}}{\partial Y^2} \right] + Ra \text{Pr} \theta - Ha^2 \text{Pr} \frac{\partial \bar{\psi}}{\partial Y} \end{array} \right\} dXdY$$

(3.11)

where R^e is the residue.

Considering the terms individually

$$\int_A [N]^T \frac{\partial \bar{\psi}}{\partial Y} \frac{\partial^2 \bar{\psi}}{\partial X \partial Y} dA = \frac{1}{4A} \left\{ \begin{array}{l} c_1 \bar{\psi}_1 + c_2 \bar{\psi}_2 + c_3 \bar{\psi}_3 \\ c_1 \bar{\psi}_1 + c_2 \bar{\psi}_2 + c_3 \bar{\psi}_3 \\ c_1 \bar{\psi}_1 + c_2 \bar{\psi}_2 + c_3 \bar{\psi}_3 \end{array} \right\} [b_1, b_2, b_3]$$

(3.12)

$$\int_A [N]^T \frac{\partial \bar{\psi}}{\partial X} \frac{\partial^2 \bar{\psi}}{\partial Y^2} dA = \frac{1}{12A} \left\{ \begin{array}{l} b_1 \bar{\psi}_1 + b_2 \bar{\psi}_2 + b_3 \bar{\psi}_3 \\ b_1 \bar{\psi}_1 + b_2 \bar{\psi}_2 + b_3 \bar{\psi}_3 \\ b_1 \bar{\psi}_1 + b_2 \bar{\psi}_2 + b_3 \bar{\psi}_3 \end{array} \right\} [c_1, c_2, c_3]$$

(3.13)

$$\int_A [N^T] \gamma \frac{\partial^2 \bar{\psi}}{\partial Y^2} \frac{\partial \bar{\psi}}{\partial X} dA = \frac{\gamma}{12A} \begin{Bmatrix} b_1 \bar{\psi}_1 + b_2 \bar{\psi}_2 + b_3 \bar{\psi}_3 \\ b_1 \bar{\psi}_1 + b_2 \bar{\psi}_2 + b_3 \bar{\psi}_3 \\ b_1 \bar{\psi}_1 + b_2 \bar{\psi}_2 + b_3 \bar{\psi}_3 \end{Bmatrix} [c_1, c_2, c_3] \quad (3.14)$$

$$\int_A [N^T] \gamma \frac{\partial^2 \bar{\psi}}{\partial Y^2} dA = -\frac{\gamma}{4A} \begin{bmatrix} b_1^2 & b_1 b_2 & b_1 b_3 \\ b_1 b_2 & b_2^2 & b_2 b_3 \\ b_1 b_3 & b_2 b_3 & b_3^2 \end{bmatrix} \begin{bmatrix} \theta_1 \\ \theta_2 \\ \theta_3 \end{bmatrix} \quad (3.15)$$

$$\int_A [N^T] \text{Pr} \frac{\partial^2 \bar{\psi}}{\partial X^2} dA = -\frac{\text{Pr}}{4A} \begin{bmatrix} c_1^2 & c_1 c_2 & c_1 c_3 \\ c_1 c_2 & c_2^2 & c_2 c_3 \\ c_1 c_3 & c_2 c_3 & c_3^2 \end{bmatrix} \begin{bmatrix} \theta_1 \\ \theta_2 \\ \theta_3 \end{bmatrix}$$

$$\int_A [N^T] \text{Pr} \frac{\partial^2 \bar{\psi}}{\partial Y^2} dA = -\frac{\text{Pr}}{4A} \begin{bmatrix} b_1^2 & b_1 b_2 & b_1 b_3 \\ b_1 b_2 & b_2^2 & b_2 b_3 \\ b_1 b_3 & b_2 b_3 & b_3^2 \end{bmatrix} \begin{bmatrix} \theta_1 \\ \theta_2 \\ \theta_3 \end{bmatrix} \quad (3.16)$$

$$\int_A [N]^T RaP \theta dA = \frac{RaP}{12A} \begin{bmatrix} \theta_1 \\ \theta_2 \\ \theta_3 \end{bmatrix} \quad (3.17)$$

$$\int_A [N^T] Ha^2 \text{Pr} \frac{\partial \bar{\psi}}{\partial Y} dA = \frac{Ha^2 \text{Pr}}{4A} \begin{bmatrix} b_1^2 & b_1 b_2 & b_1 b_3 \\ b_1 b_2 & b_2^2 & b_2 b_3 \\ b_1 b_3 & b_2 b_3 & b_3^2 \end{bmatrix} \begin{bmatrix} \theta_1 \\ \theta_2 \\ \theta_3 \end{bmatrix} \quad (3.17)$$

Thus the whole equation (3.10) can be written in matrix form as

$$\begin{aligned}
 & \frac{1}{4A} \begin{Bmatrix} c_1 \bar{\psi}_1 + c_2 \bar{\psi}_2 + c_3 \bar{\psi}_3 \\ c_1 \bar{\psi}_1 + c_2 \bar{\psi}_2 + c_3 \bar{\psi}_3 \\ c_1 \bar{\psi}_1 + c_2 \bar{\psi}_2 + c_3 \bar{\psi}_3 \end{Bmatrix} [b_1, b_2, b_3] - \frac{1}{12A} \begin{Bmatrix} b_1 \bar{\psi}_1 + b_2 \bar{\psi}_2 + b_3 \bar{\psi}_3 \\ b_1 \bar{\psi}_1 + b_2 \bar{\psi}_2 + b_3 \bar{\psi}_3 \\ b_1 \bar{\psi}_1 + b_2 \bar{\psi}_2 + b_3 \bar{\psi}_3 \end{Bmatrix} [c_1, c_2, c_3] \\
 & + \frac{\gamma}{12A} \begin{Bmatrix} b_1 \bar{\psi}_1 + b_2 \bar{\psi}_2 + b_3 \bar{\psi}_3 \\ b_1 \bar{\psi}_1 + b_2 \bar{\psi}_2 + b_3 \bar{\psi}_3 \\ b_1 \bar{\psi}_1 + b_2 \bar{\psi}_2 + b_3 \bar{\psi}_3 \end{Bmatrix} [c_1, c_2, c_3] + \frac{\gamma}{4A} \begin{bmatrix} b_1^2 & b_1 b_2 & b_1 b_3 \\ b_1 b_2 & b_2^2 & b_2 b_3 \\ b_1 b_3 & b_2 b_3 & b_3^2 \end{bmatrix} \begin{bmatrix} \theta_1 \\ \theta_2 \\ \theta_3 \end{bmatrix} \\
 & - \frac{\text{Pr}}{4A} \begin{bmatrix} c_1^2 & c_1 c_2 & c_1 c_3 \\ c_1 c_2 & c_2^2 & c_2 c_3 \\ c_1 c_3 & c_2 c_3 & c_3^2 \end{bmatrix} \begin{bmatrix} \theta_1 \\ \theta_2 \\ \theta_3 \end{bmatrix} + \frac{\text{Pr}}{4A} \begin{bmatrix} b_1^2 & b_1 b_2 & b_1 b_3 \\ b_1 b_2 & b_2^2 & b_2 b_3 \\ b_1 b_3 & b_2 b_3 & b_3^2 \end{bmatrix} \begin{bmatrix} \theta_1 \\ \theta_2 \\ \theta_3 \end{bmatrix} \\
 & + \frac{RaP}{12A} \begin{bmatrix} \theta_1 \\ \theta_2 \\ \theta_3 \end{bmatrix} - \frac{Ha^2 \text{Pr}}{4A} \begin{bmatrix} b_1^2 & b_1 b_2 & b_1 b_3 \\ b_1 b_2 & b_2^2 & b_2 b_3 \\ b_1 b_3 & b_2 b_3 & b_3^2 \end{bmatrix} \begin{bmatrix} \theta_1 \\ \theta_2 \\ \theta_3 \end{bmatrix} = 0
 \end{aligned} \tag{3.18}$$

(3.18)

Introducing stream function, the energy equation (3.7) reduces as

$$\frac{\partial \bar{\psi}}{\partial Y} \frac{\partial \theta}{\partial X} + \frac{\partial \bar{\psi}}{\partial X} \frac{\partial \theta}{\partial Y} = \left(\frac{\partial^2 \theta}{\partial X^2} + \frac{\partial^2 \theta}{\partial Y^2} \right) \tag{3.19}$$

FEM of Energy Equation is

$$\{R^e\} = - \int_A [N]^T \left(\frac{\partial \bar{\psi}}{\partial Y} \frac{\partial \theta}{\partial X} + \frac{\partial \bar{\psi}}{\partial X} \frac{\partial \theta}{\partial Y} - \frac{\partial^2 \theta}{\partial X^2} - \frac{\partial^2 \theta}{\partial Y^2} \right) dA \tag{3.20}$$

Considering the terms individually

$$\int_A [N]^T \frac{\partial \bar{\psi}}{\partial Y} \frac{\partial \theta}{\partial X} dA = \frac{1}{12A} \begin{Bmatrix} c_1 \bar{\psi}_1 + c_2 \bar{\psi}_2 + c_3 \bar{\psi}_3 \\ c_1 \bar{\psi}_1 + c_2 \bar{\psi}_2 + c_3 \bar{\psi}_3 \\ c_1 \bar{\psi}_1 + c_2 \bar{\psi}_2 + c_3 \bar{\psi}_3 \end{Bmatrix} [b_1, b_2, b_3] \begin{bmatrix} \theta_1 \\ \theta_2 \\ \theta_3 \end{bmatrix} \tag{3.21}$$

$$\int_A [N]^T \frac{\partial \bar{\psi}}{\partial X} \frac{\partial \theta}{\partial Y} dA = \frac{1}{12A} \begin{Bmatrix} b_1 \bar{\psi}_1 + b_2 \bar{\psi}_2 + b_3 \bar{\psi}_3 \\ b_1 \bar{\psi}_1 + b_2 \bar{\psi}_2 + b_3 \bar{\psi}_3 \\ b_1 \bar{\psi}_1 + b_2 \bar{\psi}_2 + b_3 \bar{\psi}_3 \end{Bmatrix} [c_1, c_2, c_3] \begin{bmatrix} \theta_1 \\ \theta_2 \\ \theta_3 \end{bmatrix} \tag{3.22}$$

$$\int_A [N^T] \frac{\partial^2 \theta}{\partial X^2} dA = -\frac{1}{4A} \begin{bmatrix} b_1^2 & b_1 b_2 & b_1 b_3 \\ b_1 b_2 & b_2^2 & b_2 b_3 \\ b_1 b_3 & b_2 b_3 & b_3^2 \end{bmatrix} \begin{bmatrix} \theta_1 \\ \theta_2 \\ \theta_3 \end{bmatrix} \quad (3.23)$$

$$\int_A [N^T] \frac{\partial^2 \theta}{\partial Y^2} dA = -\frac{1}{4A} \begin{bmatrix} c_1^2 & c_1 c_2 & c_1 c_3 \\ c_1 c_2 & c_2^2 & c_2 c_3 \\ c_1 c_3 & c_2 c_3 & c_3^2 \end{bmatrix} \begin{bmatrix} \theta_1 \\ \theta_2 \\ \theta_3 \end{bmatrix} \quad (3.24)$$

Thus the whole equation (3.19) can be written in matrix form as

$$\begin{aligned} & \frac{1}{12A} \begin{Bmatrix} c_1 \bar{\psi}_1 + c_2 \bar{\psi}_2 + c_3 \bar{\psi}_3 \\ c_1 \bar{\psi}_1 + c_2 \bar{\psi}_2 + c_3 \bar{\psi}_3 \\ c_1 \bar{\psi}_1 + c_2 \bar{\psi}_2 + c_3 \bar{\psi}_3 \end{Bmatrix} [b_1, b_2, b_3] \begin{bmatrix} \theta_1 \\ \theta_2 \\ \theta_3 \end{bmatrix} - \frac{1}{12A} \begin{Bmatrix} b_1 \bar{\psi}_1 + b_2 \bar{\psi}_2 + b_3 \bar{\psi}_3 \\ b_1 \bar{\psi}_1 + b_2 \bar{\psi}_2 + b_3 \bar{\psi}_3 \\ b_1 \bar{\psi}_1 + b_2 \bar{\psi}_2 + b_3 \bar{\psi}_3 \end{Bmatrix} [c_1, c_2, c_3] \begin{bmatrix} \theta_1 \\ \theta_2 \\ \theta_3 \end{bmatrix} \\ & - \frac{1}{4A} \begin{bmatrix} b_1^2 & b_1 b_2 & b_1 b_3 \\ b_1 b_2 & b_2^2 & b_2 b_3 \\ b_1 b_3 & b_2 b_3 & b_3^2 \end{bmatrix} \begin{bmatrix} \theta_1 \\ \theta_2 \\ \theta_3 \end{bmatrix} + \frac{1}{4A} \begin{bmatrix} c_1^2 & c_1 c_2 & c_1 c_3 \\ c_1 c_2 & c_2^2 & c_2 c_3 \\ c_1 c_3 & c_2 c_3 & c_3^2 \end{bmatrix} \begin{bmatrix} \theta_1 \\ \theta_2 \\ \theta_3 \end{bmatrix} = 0 \end{aligned} \quad (3.25)$$

IV. NUSSLET NUMBER

The average dimensionless Nusselt Number (\overline{Nu}) can be evaluated using the formula

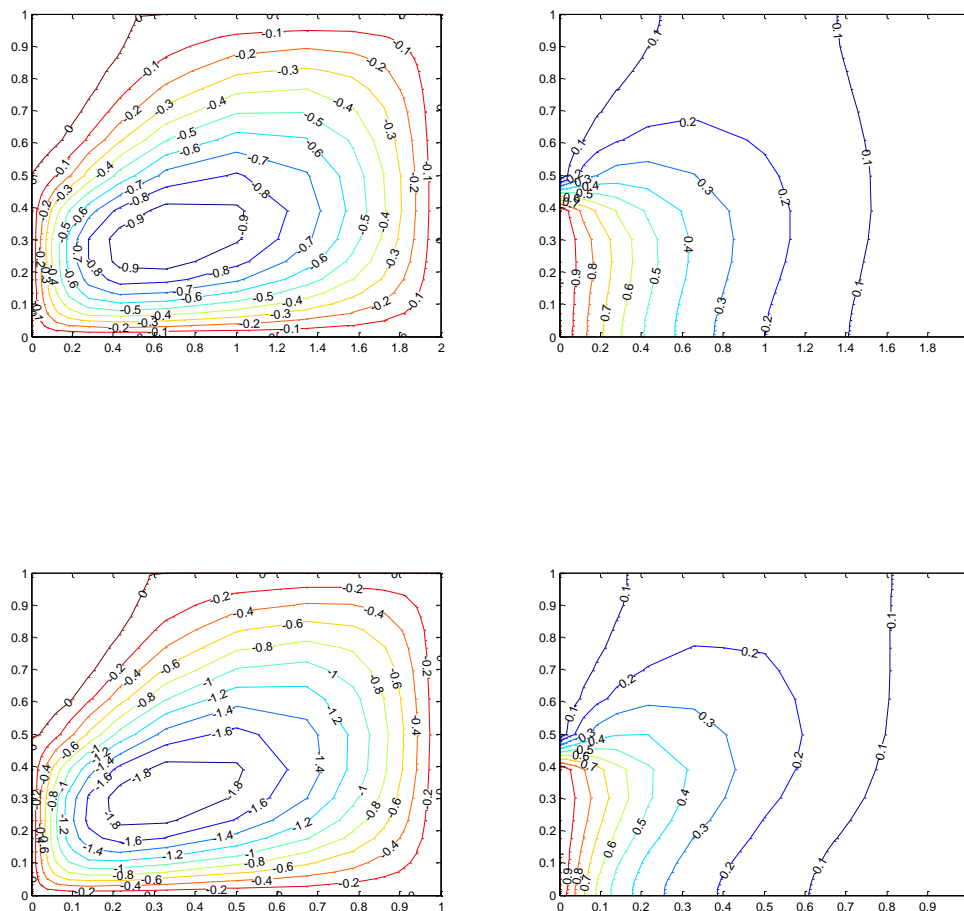
$$\overline{Nu} = -\frac{\partial \theta}{\partial n} \quad (3.26)$$

where n denotes the normal direction on a plane.

V. RESULTS AND DISCUSSION

A numerical analysis has been performed in this work to investigate the effects of magnetic field in a square cavity with a semi circular heated obstacle of different orientation parameter (rot). The ranges rot and Ha for this investigation vary from 0° to 90° and 0 to 100 respectively whereas other parameters are fixed at $\text{Ra} = 10^4$ and $\text{Pr} = 0.71$. In this section the influence of the Hartmann number ($\text{Ha} = 0, 50, 100$) on the flow and temperature fields for $\text{Ra} = 10^4$ and three values of the orientation parameter ($\text{rot} = 0^\circ, 60^\circ, 90^\circ$) are presented. Fig.4 illustrates the streamlines and isotherms for $\text{rot} = 0^\circ$, where the buoyancy effects dominate the flow field in the cavity and the heat transfer is mainly due to natural convection. The results show that the buoyancy induced vortices in the cavity in the absence of the magnetic field ($\text{Ha} = 0$). Four vortices are evident inside of the cavity for $\text{Ha} = 0$. When the Hartmann number increases, both of them are vanished due to the

effect of the magnetic field. The isotherms distribution is also affected by the effect of the magnetic field. Less bend of the isotherms lines is observed as the Hartmann number increases. Fig. 5 shows the streamlines and isotherms for $\text{rot}=600$. In the absence of the magnetic field, one vortex is appearing clearly right side of the heated body due to buoyancy force. As the Hartmann number increases size of the vortex larger and move to the top side and another vortex created on the left top corner. Bending of the isotherms lines are a lesser amount of with increasing Hartmann number. Fig. 6 shows the streamlines and isotherms for $\text{rot}=900$. In the absence of the magnetic field, elliptic size only one vortex is generated right side of the heated body due to buoyancy force. As the Hartmann number increases shape of the vortex seems to be almost circular and move to the top side and another vortex created on the left top corner. Effect of the magnetic field is also significant for isotherms lines. The average Nusselt number is plotted as a function of Hartmann number and Rayleigh number respectively as shown in Fig. 7 and Fig. 8 for five different orientation ($\text{rot} = 0^\circ, 15^\circ, 30^\circ, 45^\circ, 90^\circ$) while $\text{Pr}=0.71$. The maximum heat transfer rate is obtained for the lowest Ha . This is because the magnetic field retards the flow.



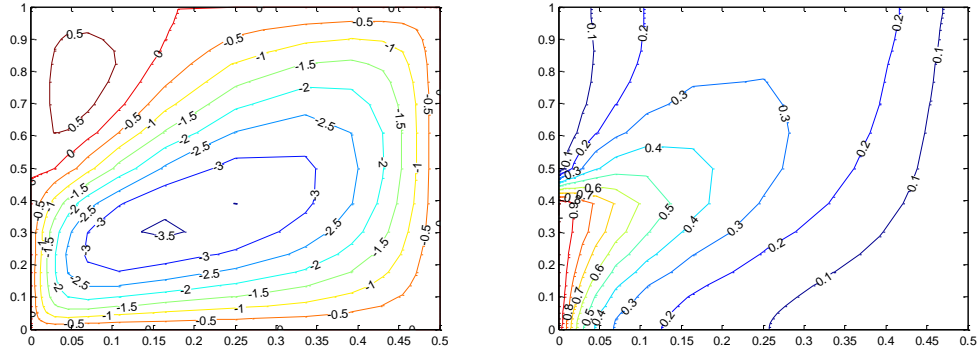


Fig. 4: Clockwise and anti-clockwise flows are shown via negative and positive signs of stream functions (Left) and Isotherms (Right) for rotation 0° with $Pr=0.71$ and

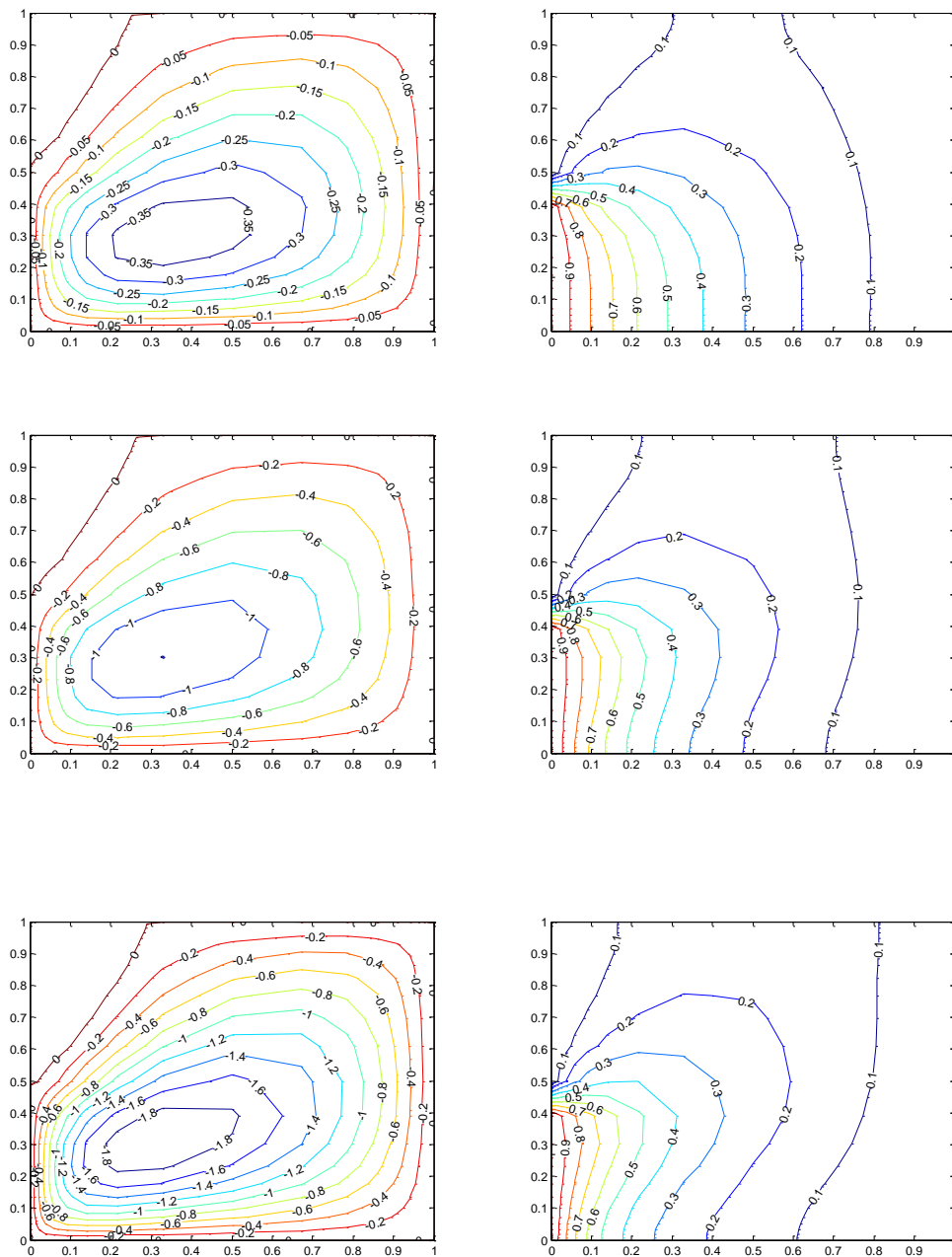


Fig.5: Clockwise and anti-clockwise flows are shown via negative and positive signs of stream functions (Left) and Isotherms (Right) for rotation 60° with $Pr=0.71$ and $Ra=10000$.

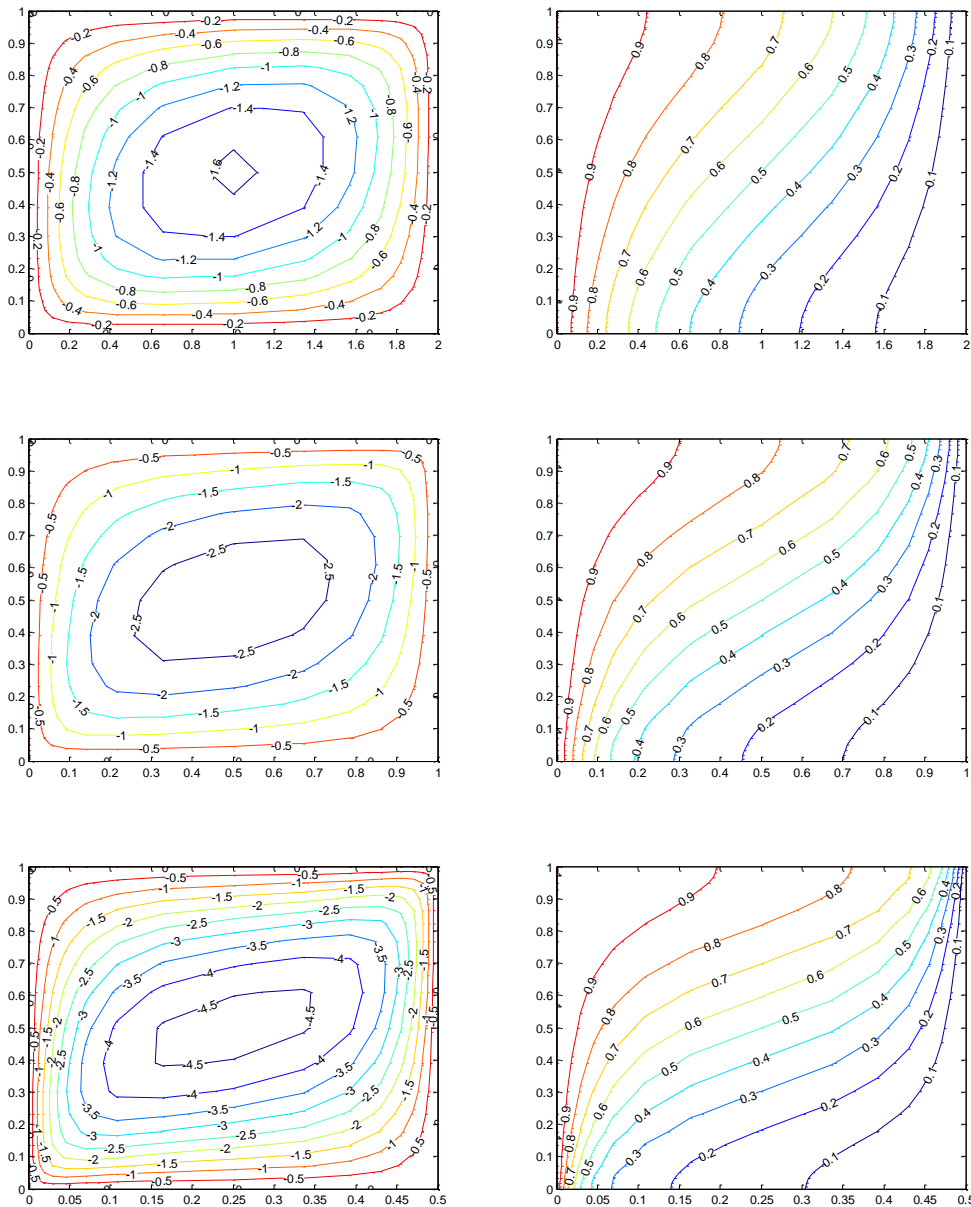


Fig.6: Clockwise and anti-clockwise flows are shown via negative and positive signs of stream functions (Left) and Isotherms (Right) for rotation 90° with $Pr=0.71$ and $Ra=10000$.

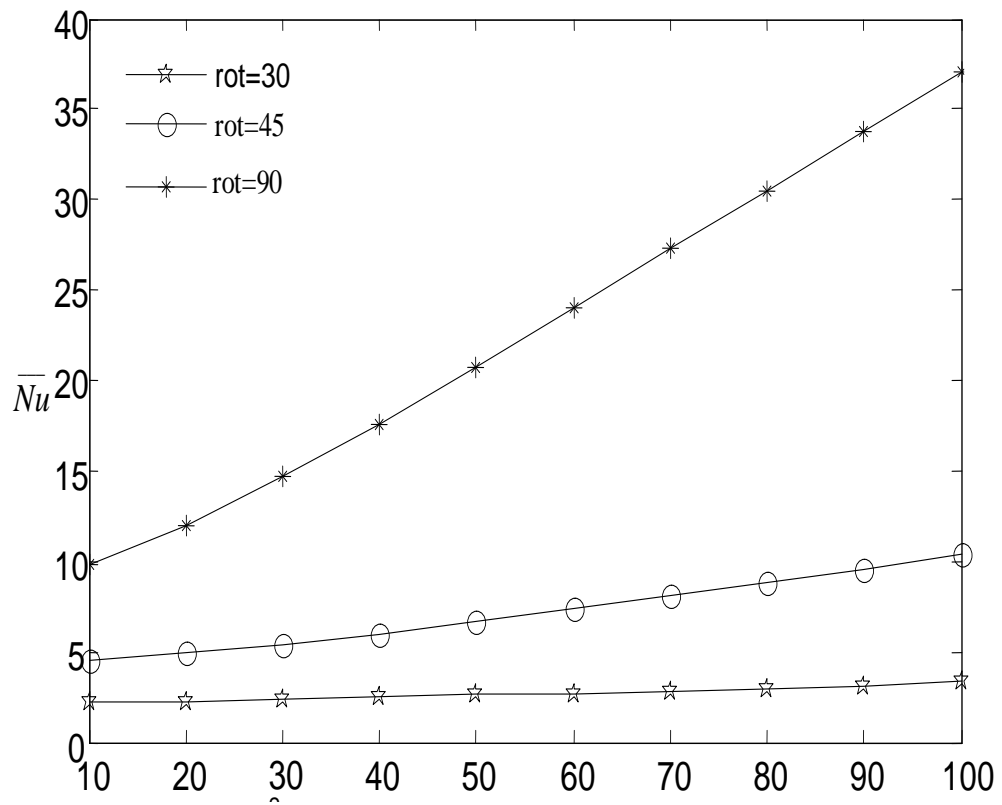


Fig. 7: Effect of Ha and rot on \bar{Nu} while $Pr=0.71$ and $Ra=10^4$

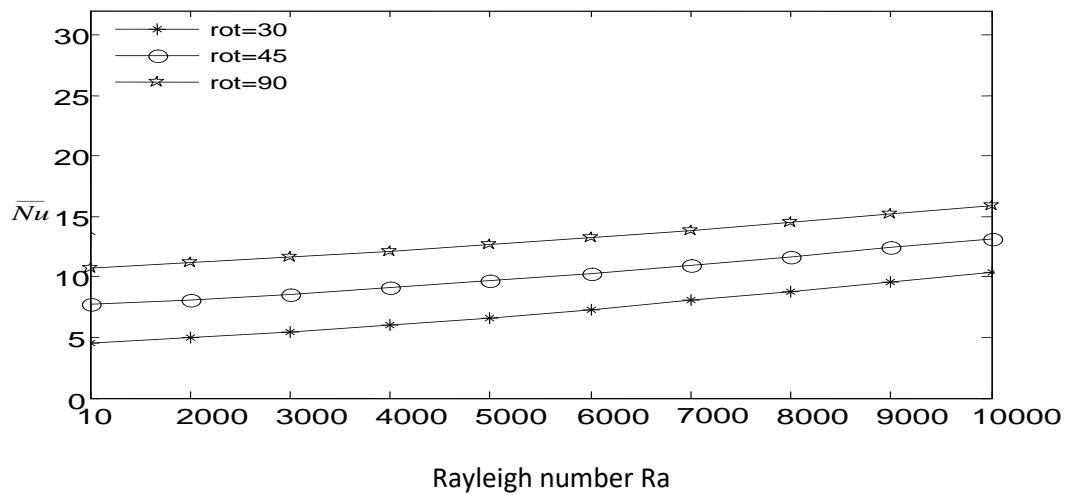


Fig.8: Effect of Ra and rot on \bar{Nu} while $Pr=0.71$ and $Ha=0$

REFERENCES

- [1]. M. A. Taghikhani, H. R. Chavoshi, Two dimensional MHD free convection with internal heating in a square cavity, *Thermal Energy and Power Engineering*, vol. 2, pp. 22-28, 2013.
- [2]. Y. Bakhshan, H. Ashoori, Analysis of a fluid behavior in a rectangular enclosure under the effect of magnetic field, *World Academy of Science, Engineering and Technology*, vol. 61, pp. 637- 641, 2012.
- [3]. F. Hakan Öztop, Khaled Al-salem, Effects of joule heating on MHD natural convection in non-isothermally heated enclosure, *J. of Thermal Science and Technology*, vol. 32, pp. 81-90, 2012.
- [4]. S. Parvin, R. Nasrin, Analysis of the flow and heat transfer characteristics for MHD free convection in an enclosure with a heated obstacle, *Nonlinear Analysis: Modeling and Control*, vol. 16, pp. 89–99, 2011.
- [5]. B. Santosh, G. Archana, Aswatha, K. N. Seetharamu, Natural convection in a square cavity localized heating from below, *The 37th National & 4th International Conference on Fluid Mechanics and Fluid Power December 16-18, 2010, IIT Madras, Chennai, India*.
- [6]. J. N. Reddy, *An introduction to Finite element method*, McGraw-Hill, New York 1993.
- [7]. VenkateswaraRaju K, Parandhama A, Raju M.C and Ramesh babuK; Unsteady MHD mixed convection flow of Jeffrey fluid past a radiating inclined permeable moving plate in the presence of thermophoresis heat generation and chemical reaction. *Journal of ultra scientist of physical sciences (JUSPS)*. Vol. 30(1), pp; 51-65 (2018).
- [8]. VenkateswaraRaju K, Parandhama A, Raju M.C, Ramesh Babu K; Unsteady MHD free convection Jeffery fluid flow of radiating and reacting past a vertical porous plate in slip-flow regime with heat source. *Frontiers in Heat and Mass Transfer (FHMT)*, 10, 25 (2018), ISSN: 2151-8629.
- [9]. Sandeep, N., and Sulochana, C., Momentum and heat transfer behaviour of Jeffrey, Maxwell and Oldroyd-B nano fluids past a stretching surface with non-uniform heat source/sink., *Ain Shams Engineering journal*, <http://dx.doi.org/10.1016/j.asej.2016.02.008> , PP:1-8, Feb, (2016).
- [10]. Malik, M.Y., Zehra, I., Nadeem, S., Numerical treatment of Jeffrey fluid with pressure-dependent viscosity, *International Journal of Numerical Methods in Fluids*, 68, 196-209 (2012).
- [11]. Qasim, M., Heat and mass transfer in a Jeffrey fluid over a stretching sheet with heat source/sink. *Alexandria journal of Engineering*, 52, 571-5 (2013).
- [12]. Obulesu M, Dastagiri Y, Siva Prasad R; Radiation absorption and chemical reaction effects on mhd radiative heat source/sink fluid past a vertical porous plate, *Journal of Engineering Research and Application* , ISSN : 2248-9622 Vol. 9, Issue 5 (Series -II) May 2019, PP: 77-87.
- [13]. Mohapatra R, Pattanayak H , Mishra S.R. : Effect of Chemical Reaction on MHD Micropolar Fluid Flow on a Vertical Surface through Porous Media with Heat Source. *International Journal of Innovative Research in Science, Engineering and Technology* , Vol. 4, Issue 9, 2015.
- [14]. Srinivas Reddy D; Impact of Chemical Reaction on MHD Free Convection Heat and Mass Transfer from Vertical Surfaces in Porous Media Considering Thermal Diffusion and Diffusion Thermo Effects. *Pelagia Research Library Advances in Applied Science Research*, 2016, 7(4), PP:235-242.
- [15]. Sheri Siva Reddy and MD. Shamshuddin; Diffusion-thermo and chemical reaction effects on an unsteady mhd free convection flow in a micropolar fluid ; *theoretical and applied mechanics volume 43 (2016) issue 1*, 117–131.
- [16]. Malik M. Y. and Khalil-ur-Rehman: Effects of Second Order Chemical Reaction on MHD Free Convection Dissipative Fluid Flow past an Inclined Porous Surface by way of Heat Generation: *Inf. Sci. Lett.* 5, No. 2, 35-45 (2016).
- [17]. Obulesu M, Siva Prasad R.; Hall Current Effects on MHD Convective Flow Past A Porous Plate with Thermal Radiation, Chemical Reaction and Heat Generation /Absorption , *To Physics Journal vol 2 (2019) ISSN: 2581-7396*.
- [18]. DileepKumar I, SinghA.K. : Effects of heat source/sink and induced magnetic field on natural convective flow in vertical concentric annuli. *Alexandria Engineering journal*, Volume 55, Issue 4 ,Pages 3037-3362 (December 2016).
- [19]. Rathod V. P., Sanjeevkumar D. : Effect of heat source/sink on the peristaltic flow of jeffrey fluid with suspended nanoparticles in an asymmetric channel having flexible walls. *International Journal of Mathematical Archive-7(10)*, 2016, 80-94 .
- [20]. Sravanthi, C. S. Gorla R. S. R. : Effects of Heat Source/Sink and Chemical Reaction on MHD Maxwell Nanofluid Flow Over a Convectively Heated Exponentially Stretching Sheet Using Homotopy Analysis Method. *International Journal of Applied Mechanics and Engineering*, Volume 23, Issue 1, pp.137-159,(2018).